Mechanistical insights into the bioconjugation reaction of Triazolinediones with tyrosine

Dustin Kaiser[1], Johan M. Winne[2], Maria Ortiz-Soto[3], Jürgen Seibel[3], Thien A. Le[1], Bernd Engels[1]*

1: Institute of physical and theoretical chemistry, Julius-Maximilans Universität Würzburg
2: Department of Organic and Macromolecular Chemistry, Ghent University
3: Institute of organic chemistry, Julius-Maximilians Universität Würzburg
* Bernd.engels@uni-wuerzburg.de

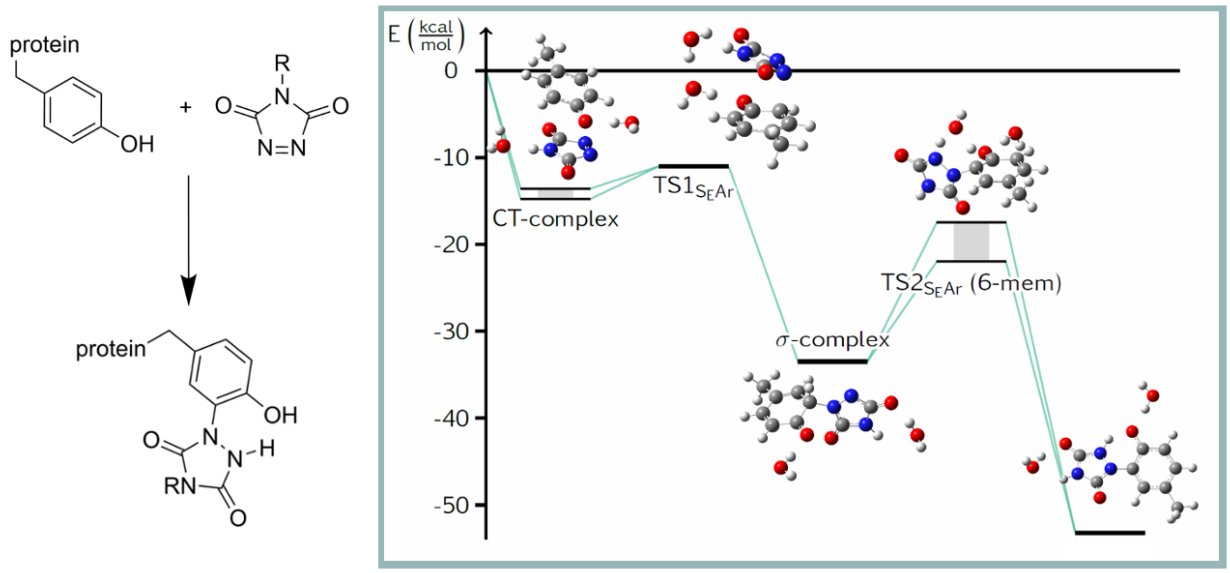

Abstract

The bioconjugation at tyrosine residues using cyclic diazodicarboxamides, especially 4-substituted-3H-1,2,4-triazole-3,5(4H)-dione (PTAD), is a highly enabling synthetic reaction because it can be employed for orthogonal and site-selective (multi)functionalizations of native peptides and proteins. Despite its importance, the underlying mechanisms have not been thoroughly investigated. Formally, the reaction can proceed along four distinctive pathways: (i) the S_EAr path, (ii) along a pericyclic group transfer pathway (a classical ene-reaction), (iii) along a step-wise reaction path, or (iv) along an unusual higher order concerted pericyclic mechanism. The product mixtures obtained from reactions of PTAD with 2,4-unsubstituted phenolate support the S_EAr mechanism, as ortho and para isomers are observed, but it remains unclear if other mechanisms take place for the protonated species usually present in proteins. In the present work the various mechanisms *in vacuo*, and in solvents are compared using high-level quantum chemistry approaches for the model reaction of 4*H*-3*H*-1,2,4-triazole-3,5(4*H*)-dione (HTAD) with *p*-cresol and *p*-cresolate. The computations of the reaction of *p*-cresol and HTAD *in vacuo* predict that the reaction barriers of the pericyclic ene-reactions are strongly favored over both the S_EAr mechanism and the step-wise biradical pathways (>10 kcal/mol). In a protic solvent (water), the barriers of the S_EAr

mechanism are predicted to be lowered, lying close to the ones of the ene-reaction. Nevertheless, the calculated reaction barriers are still too high to explain the available experimental observations. This is only possible if the S_EAr reaction of cresolate with HTAD is taken into account. For this reaction nearly vanishing barriers are computed, predicting very fast reactions of even transient amounts of deprotonated phenol species. Minding the fast decomposition of PTAD in water, this model satisfactorily explains the measured conversion rates in buffered aqueous solutions and the strong activation effects observed upon addition of bases.

Introduction

Triazolinediones, as for example 4-phenyl-3H-1,2,4triazole-3,5(4H)-dione (PTAD) are very useful reagents in chemistry which are used in thermo-[1-16] as well as photochemical reactions[17-21]. PTAD is also an important tool for mass spectrometry analysis, for example for identifying fatty acids.[22-23] In 2009, Barbas III and coworkers extended the application range of cyclic diazodicarboxamides. They published the first report of selective bioconjugation at native tyrosine residues of proteins using cyclic diazodicarboxamides, specifically 4-phenyl-3H-1,2,4triazole-3,5(4H)-dione (PTAD).[24] They could show that the reaction is highly selective for tyrosine, up to the extent that it can be employed for orthogonal and site-selective multifunctionalizations.[24-25] Since then this click-like reaction involving triazolinediones has proven to be a promising approach, as it has been employed in biorthogonal bioconjugation[25-27] as well as in macromolecular sciences.[28] Furthermore, the tyrosine click-reaction with TADs has been used to prepare DNA-protein conjugates, to couple drugs to monoclonal antibodies and to prepare glycoconjugates.[29] It was recently shown that diazodicarboxyamide bioconjugation can also be used to redesign and tailor the enzyme levansucrase for the synthesis of novel polysaccharides.[30]

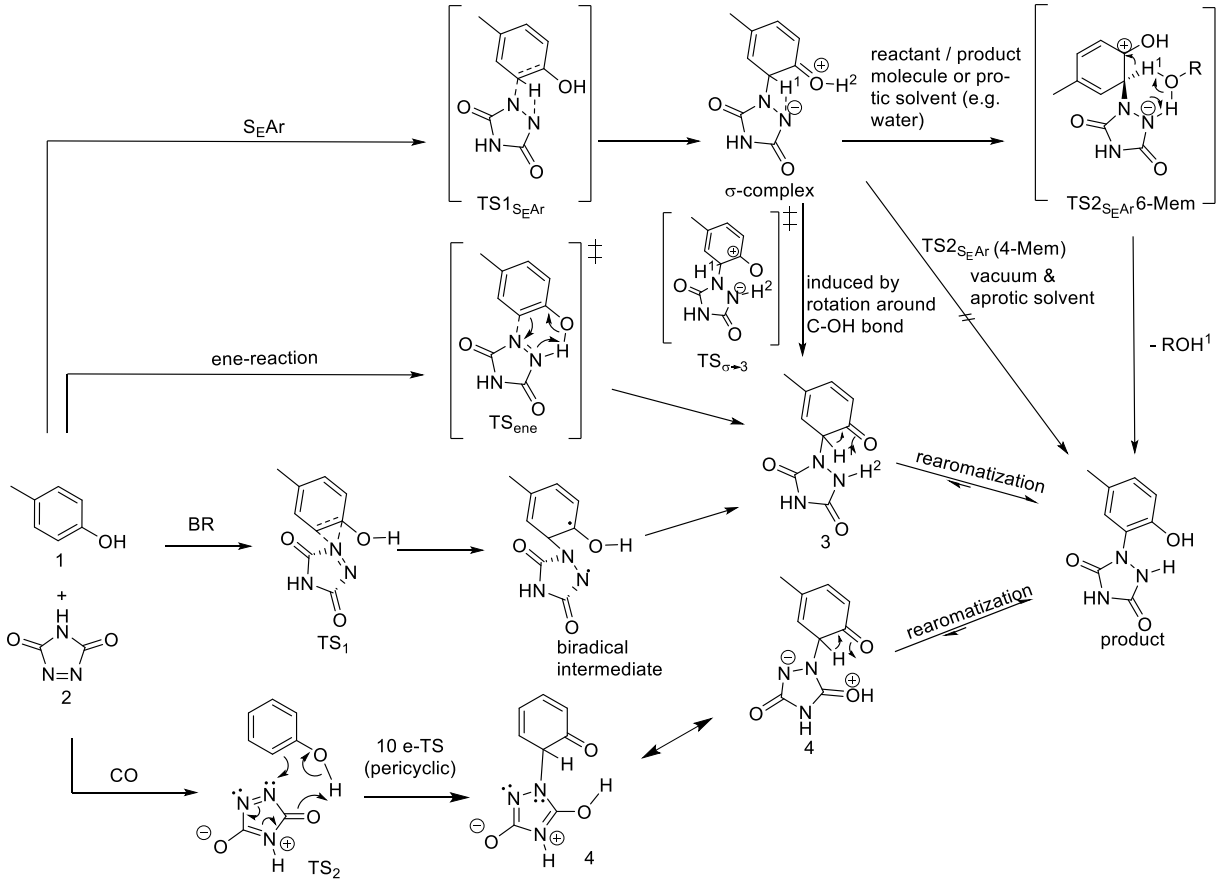

Figure 1: Summary of possible reaction pathways for the reaction of p-cresol (**1**) and HTAD (**2**).

Despite its importance, the mechanism of the reaction between PTAD and tyrosine residues was not investigated in detail, e.g. theoretical characterizations are missing to the best of our knowledge. The most recent discussion about TAD reactions is the comprehensive review by De Bruycker *et al*.[29] Therein, as in the original report of Barbas III, the TAD reaction with phenols is denoted as an 'ene reaction' but no detailed discussion (or speculation) about its possible mechanistic steps is provided. Tyrosine derivatives react rapidly (complete in 5 min) with 3 equiv. of PTAD in sodium phosphate buffer with pH=7 and a 1:1 mixture with acetonitrile. There are several key experimental observations that are indicative of significant mechanistic effects that deserve a close investigation. Importantly, the reaction between TAD reagents and phenols in organic solvents is exceedingly slow. For peptide or protein conjugations, TADs are more reactive with free amines and tryptophan residues. In aqueous medium, the adduct formation of TAD and phenols is also not efficient, and is for example outcompeted by background reactions such as a slow hydrolysis of TAD.[31] Interestingly, the reaction of phenols and TADs in buffered aqueous media (pH 7-10), is remarkably and selectively accelerated (compared to other nucleophiles which do not show this solvent dependence).[24] This key finding led Barbas III to investigate the use of TADs as selective covalent labeling reagents for tyrosine residues on protein and peptide substrates in aqueous buffers. Plausible reaction mechanisms are indicated in Figure 1, employing *p*-cresol as a model compound for the reaction of tyrosine with 4H-1,2,4triazole-3,5(4H)-dione (HTAD). The reaction might proceed via an electrophilic aromatic substitution reaction (S_EAr). In a first step, the σ-complex is formed in which the positive charge can be delocalized over the aromatic ring, while the negative charge at the PTAD-fragment is stabilized through the carbonyl-bond. In vacuum, the proton transfer to the final product has to occur by means of an energetically unfavorable four-membered ring. In solution, rearomatisation should be readily

mediated by another reactant, a solvent molecule or product species. For example, a cresol molecule could act as a bridge to form a six-membered ring for the isomerization. Furthermore, the proton transfer could result from two consecutive intermolecular acid/base reactions. Overall, the barriers for such tautomerizations are enthalpically very feasible although the reaction rate will depend on the concentration of reactant and product. For protic solvents (e.g. water) the proton-transfer can proceed along a six-membered ring including one solvent molecule. Thereby, the timescale of the rearomatisation is expected to become independent of the concentration of reactant and product. In addition to the standard S_EAr reaction path the σ-complex can also pass to the intermediate **3** by an internal proton transfer from the positively charged OH-group to the negatively charged nitrogen. This transfer would proceed through a six-membered transition state as indicated in Figure 1.

For *p*-cresol and TADs, a pericyclic group transfer pathway (pericyclic ene-reaction) which proceeds along a highly ordered six-membered transition state (TS_{ene}) is also possible. The concerted step leads to the same intermediate adduct **3,** which then can readily tautomerize to the favored aromatic isomer. The pathways for this tautomerization is determined by similar effects as discussed for the rearomatization of the σ-complex to the product and is expected to be very feasible under ambient conditions. For the reaction of PTAD with alkenes such a concerted ene-reaction was not found[32] but Lu reported the first concerted nitroso ene-reaction that occurs between *o*-isotoluene and nitroso compounds.[33]

Beside the mechanisms described above, two further mechanisms are conceivable. The first one (BR) resembles the now classical mechanism for TAD ene-reactions, which was found by Houk and coworkers[32, 34] for the reactions of HTAD with propene. For propene, the mechanism proceeds *via* formation of a biradical intermediate. This intermediate then reacts again to the previously described intermediate **3** *via* a 1,5-hydrogen shift. In a last mechanism, HTAD is attacked by cresol, but the hydrogen is not transferred to the second nitrogen center but relayed to the carbonyl group neighboring to the electrophilic nitrogen center (CO mechanism). Through a kind of pericyclic 10 e-TS[35-37] the proton transfer leads to intermediate **4**. The final product is obtained from **4** by a double tautomerization reaction. This mechanism is quite unusual but was already discussed by Houk for the reaction of HTAD with propene.[32]

Previous experimental findings of Barbas III and co-workers indicate that the S_EAr mechanism most likely takes place.[24, 38] While conversions to the product were found for aqueous buffered solutions (NaH_2PO_4-Na_2HPO_4-MeCN buffer, pH 7-7.4) no reactions is found if MeCN or a mixture of MeCN and H_2O (1:1) are taken as solvents. Additionally, further literature showed that the reaction also takes place for phenolate for which no ene-reaction is possible.[39] Nevertheless, the experiments do not exclude competing mechanisms in different environments.

To shed some light on this important topic, we computed the various possible mechanisms for the reaction of *p*-cresol with HTAD for different environments in the present work. Beside vacuum calculations, we also included the influence of a polarizable environment through the polarizable continuum model (PCM). In addition, we characterized the influence of explicit solvent effects by adding water molecules. Water may catalyze the S_EAr path considerably because of its hydrogen bond donating capacity (Figure 1). In order to ensure that the mechanisms are described on equal footing we employed CCSD(T) as well as CASPT2 beside DFT. The multi-reference approach CASPT2 was used because the intermediates of the stepwise reaction of HTAD with propene possessed severe biradical character.[40] We mainly report CCSD(T) energetics in this report while comprehensive results of all computational methods can be found in the accompanying Supporting Information (SI). Using these high-level approaches as benchmark, we investigated the applicability of the density functional approach. We extended the investigation towards the reactions of the cresolate anion to study how a basic environment influences the barriers of the S_EAr mechanism. In order to investigate which effects determine the energetics, we

studied the influence of the aromatic system of cresol by comparing its reaction with the corresponding reactions of vinyl alcohol. For the reaction of TADs with xylene, mesitylene, or anisole Breton and Hoke have recently provided conclusive evidence that a radical mechanism takes place.[19, 41] To elucidate possible differences between -OH and $-CH_3$ substituents, we further compared the reactions of HTAD with vinyl alcohol and propene.

Computational Methods

All geometries were obtained at the B3LYP[42-44]/aug-cc-pVDZ[45] and ωB97xD[46]/aug-cc-pVDZ[45] level of theory using the Gaussian09 Rev. E software package.[47] For ωB97xD optimizations, structures have previously been optimized at the B3LYP/aug-cc-pVDZ level of theory. In the case of the TAD ene-reaction with *p*-cresol and vinyl-alcohol, the B3LYP potential energy surface (PES) includes superfluous stationary geometries near transition states. This failure of B3LYP for some organic chemical reactions has previously been reported.[48-49]

For all stationary geometries, frequency calculations were performed to validate them as true minima or first-order saddle points of the PES. For transition-states, intrinsic reaction coordinate (IRC) calculations were performed to find the minima connected by the transition state. All energy calculations at the ωB97xD, MP2 and CCSD(T) level of theory were performed using Gaussian09. $\mathcal{T}_1$ diagnostics have been obtained from converged CCSD amplitudes.[50] Single reference approaches are often sufficiently accurate, however in some cases multi-reference approaches are needed to obtain accurate PES,[51] electronically excited states or even properties.[52] Based on the previous studies of Houk and co-worker for the present study multi-reference effects could be expected to be important.[32] Hence, we used the Complete Active Space (CAS) approach in which dynamic correlation effects are taken into account in second order perturbation theory (PT2).[53-54] All CASPT2 calculations were performed using the MOLCAS 7.8 program package.[55] The active space of the CASPT2(14,14) calculations was built iteratively starting from canonical HF orbitals in the [4,4] case and building larger CAS spaces from pseudo-natural average orbitals of each smaller CI space. The energies of separated reactants were calculated for both molecules spaced more than 10 Å apart in the case of CASPT2 calculations. Solvent effects were included using the Polarizable Continuum Model (PCM), as implemented in Gaussian09 Rev. E and MOLCAS 7.8. For the CT states and all intermediates we checked for alternating open-shell species using unrestricted singlet and triplet optimizations at the ωB97xD[46]/aug-cc-pVDZ[45] level of theory. In no case relevant open-shell species were observed. Details regarding the influence of the considered open-shell structures are found in Table S7 in the SI.

Results and Discussion

As a first step, we investigated possible paths of the reaction of *p*-cresol with HTAD which are summarized in Figure 1. Within this search, which was performed on the ωB97xD/aug-cc-pVDZ level of theory, we could indeed identify the corresponding stationary points of all four different mechanisms. The geometries of the various stationary points are given in the Figures S1, S2, S3, and S4. Additional single points energy differences of these geometries were computed using CCSD(T) and CASPT2 to elucidate the influence of the theoretical approach on the relative energies (see first column of Table 1 and Table S4 in the SI). All energies are given with respect to the separated reactants. For CASPT2, which is not strictly size consistent,[56] the reactants were computed within a distance of 10 Å.

Our calculations indicate that the fragments form a stable pre-reactive complex. To check the accuracy of this binding event, we computed the basis set superposition error (BSSE). It is only about 1 kcal/mol at the ωB97xD/aug-cc-pVDZ and 5.5 kcal/mol on the CCSD(T)/aug-cc-pVDZ level of theory, showing that the binding is not an artifact of the calculation. To investigate if this complex corresponds to the charge-

transfer (CT) complex described previously by Breton and co-workers,[18-19] and also by other groups,[6, 57] we computed its lowest lying electronically excited states for polar media employing PCM. These computations were performed using the TDDFT approach at the ωB97xD/aug-cc-pVDZ level of theory because range-separated functionals are needed for the description of CT states.[58-60] This level of theory predicted electronically excited states at 469 and 425 nm and various states between 350-320 nm with quite low or vanishing transition dipole moments. Taking the standard error of 0.1 – 0.2 eV into account these findings agree nicely with the broad band (430 – 350 nm) described by Breton and Hoke for MeTAD and substituted benzenes. Hence, in the following passages this complex is named CT-complex and the discussion will mainly focus on the relative energies with respect to this CT state. It is formed without any barrier and due to the subsequent high reaction barriers, its lifetime is sufficiently long for the binding energy to be dissipated before the reaction takes place. The binding of the CT state mainly results due to dispersion effects as shown by comparing the binding energies obtained with B3LYP/aug-cc-pVDZ (0.9 kcal/mol) and with B3LYP-D3/aug-cc-pVDZ (7.6 kcal/mol). This is in line with previous investigations of Scheiner and co-workers.[61] It should also be noted that due to the computed basis set superposition error (BSSE) the relative heights of the reaction barriers are overestimated by 1-5 kcal/mol depending on the theoretical approach.

	CCSD(T) *in vacuo*	**CCSD(T) + PCM**	**CCSD(T) + PCM + H_2O**
CT-complex	-12.1	-10.0	[2] -9.3 / [4] -8.8
$TS1_{S_EAR}$	16.2 (28.3)	14.4 (24.4)	14.4 (23.2)
σ-complex	16.2 (28.3)	12.6 (22.6)	11.3 (20.1)
$TS_{\sigma \rightarrow 3}$	8.2 (20.3)	22.7 (32.7)	21.7 (30.5)
$TS2_{S_EAR}$ (4-mem)	[1] n.c.	[1] n.c.	[1] n.c.
$TS2_{S_EAR}$ (6-mem)	---	---	[2] 8.1 (17.4) / [3] 14.8 (23.6)
TS_{ene}	14.4 (22.9)	10.8 (20.8)	11.2 (20.0)
[4] $TS_{Solvent}$	---	---	[2] 15.9 (25.2) / [3] 22.6 (31.4)
3	-24.5 (-16.0)	-20.1 (-10.1)	-18.9 (-10.1)
TS_1	27.4 (35.9)	24.8 (34.8)	24.6 (33.4)
TS_2	23.1 (31.6)	21.7 (31.7)	20.1 (28.9)
4	-0.8 (7.7)	-2.8 (8.2)	[1] n.c.
Product	-43.3 (-32.8)	-35.9 (-25.9)	-34.9 (-26.1)

[1] not computed.

[2] relative energies with respect to fragments or CT-complex which are not stabilized by a water molecule.

[3] relative stability with respect to the fragments (or CT state) which are stabilized by a water molecule.

[4] see Figure 2.

Table 1: Relative energies [kcal/mol] with respect to the fragments (to the CT-complex) of the stationary points of the various reaction paths of the reaction of HTAD with *p*-cresole. For all calculations the aug-cc-pVDZ basis sets were used. The geometries were optimized using the ωB97xD DFT

functional. In addition to the CCSD(T) results, CASPT2(14,14) and ωB97xD energetics have been calculated (see Tables S4-S6 in the SI).

All hitherto reported experimental investigations of TAD-tyrosine click reactions are performed in polar protic solutions. Nevertheless, we will briefly discuss the results obtained for vacuum conditions to see the influence of polar aprotic or protic solvent and to investigate differences to the reaction between HTAD and propene which were characterized in vacuum. In the CT-complex found for the vacuum computations, both fragments are separated by about 2.75 Å. They are in a face-to-face orientation, but slightly shifted with respect to each other so that the N=N bond of HTAD lies above the CO-bond of the cresol (see Figure S1 and Figures 3-5). The computed binding energies of the CT-complex vary between -12 kcal/mol for CCSD(T) and +5 kcal/mol for CASPT2(14,14). Due to the relative orientation of the two fragments with respect to each other two CT-complexes with different geometries are possible. In the first one the OH moiety is placed below the five-membered ring of HTAD while it is oriented away from it in the second geometry. The influence of both orientations on the reaction mechanism will discussed below because most experiments were performed in solution. In summary, our computations predict that for vacuum the pericyclic ene mechanism is energetically most favorable. The computed barrier heights (TS_{ene}) with respect to the CT-complex vary between 21 kcal/mol (CCSD(T)) and about 8 kcal/mol (CASPT2(14,14)). The differences may arise because as indicated by the $\mathcal{T}_1$-diagnostic multi-reference effects seem to be non-negligible. Similar variations are found for all other stationary states.

While the absolute values of the computed barrier heights differ, all approaches agree that the corresponding barriers for the S_EAr mechanism ($TS1_{S_EAR}$) are considerably higher than those found for the pericyclic ene-reaction (see Table S4). All approaches also agree that the barriers for the two step-wise reactions are even higher than those of the S_EAR-barriers. It is important to note that for vacuum the pericyclic ene-reaction might only proceed to the intermediate **3** because the proton transfer necessary to reach the final product will have a quite high barrier *in vacuo*. This is indicated by the failure of all our attempts to determine the corresponding transition states. We refrain from further investigations because we are mainly interested in the reactions taking place in aqueous solution.

The data given in the second column of Table 1 contains solvent effects within the framework of the PCM continuum approach which includes polarization effects but neglects molecular effects of a given solvent. The structures of the stationary points are given in Figure S2**.** In the CT-complex, with a binding energy varying between 6 and 12 kcal/mol, both fragments are separated by about 3.2 Å (see SI), i.e. the separation is slightly larger than for vacuum. The energy difference between the two possible orientations of the CT-complexes is only 0.2 kcal/mol (-6.1 vs. -6.3 kcal/mol). This could be expected because the binding energy mainly results from dispersion effects and donor/acceptor interactions which should not be influenced by the orientation of the OH-moiety. A switch from one minimum to the other minimum is possible through a rotation of the OH group towards the HTAD fragment or away from the HTAD fragment. To get insights if the transfer is a fast motion we computed the barrier of the rotation away from HTAD because the system approaches the transition state of the pericyclic ene-reaction if the OH-group is rotated towards the HTAD. The barrier of the former rotation is about 4 kcal/mol. The small barrier indicates that the resulting fast equilibrium will not influence which path is taken according to the Curtin-Hammett principle.[62]

As expected, the inclusion of solvent effects stabilizes the stationary points with a large degree of charge separation along the S_EAr pathway. In comparison to the gas phase the $TS1_{S_EAR}$ is stabilized by about 3-4 kcal/mol (relative energy with respect to the CT-complex) while the corresponding relative stabilization of the σ-complex is even larger. Starting from the σ-complex, the S_EAr mechanism can proceed along

three different paths (Figure 1). The first one proceeds along a four-membered transition state going directly to the final product. It is expected to be a very unfavorable one. Indeed, a constraint optimization procedure varying the bond length of the C-H bond of the σ-complex incrementally at the ωB97xD/aug-cc-pVDZ + PCM level of theory predict a barrier height of 36.7 kcal/mol.

The proton transfer from the formally positively charged OH moiety to the formally negatively charged nitrogen of the HTAD, which represents a connection between the σ complex and intermediate **3**, is the second pathway of the S_EAr mechanism. This route passes through a relaxed six-membered ring as indicated in Figure 1. Starting from the situation in which the proton H^2 (see Figure 1) is oriented away from the HTAD moiety the reaction is induced by a rotation of the OH-group around the CO bond. Our computations indicate that this rotation possesses a barrier of about 23 kcal/mol while the subsequent proton transfer possess no barrier. This shows that a σ-complex in which the OH group is oriented towards the HTAD will not be stable but will directly proceed to **3**. From a closer look on the orientation of the transition state of the pericyclic ene-reaction (TS_{ene} see Figure S2) it becomes clear that such an orientation of the OH-group indeed closely resembles transition state of the pericyclic ene-mechanism (see below). From **3** the final product is reached through the tautomerization from the keto- to the enol-form which will be discussed in connection with the pericyclic ene-mechanism.

As a final branch in the S_EAr mechanism, the proton transfer leading to the final product can proceed through a six-membered ring which within an aprotic solvent includes a reactant or a product molecule as bridge ($TS2_{S_EAR}$ (6-mem)). The barrier height of this proton transfer will be similar to the barrier height including water as a bridge (10-14 kcal/mol) which is shown in Table 1. This is considerably lower than the barrier height of the $TS1_{S_EAR}$ transition state (20-25 kcal/mol) so that entropic effects are not expected to shift the relative energy of the $TS2_{S_EAR}$ (6-mem) above that of the $TS1_{S_EAR}$ transition state. Considering that the final product could also be formed within two consecutive intermolecular acid/base reactions the formation of the σ-complex is predicted to be the rate determining step of the S_EAr mechanism in aprotic solvents. The energetic and structural properties of the S_EAr mechanisms which were determined for the reaction of TAD and *p*-cresol are showcased in Figure 2.

While the barrier to the σ-complex is considerably lowered by polar solvents, the barrier of the pericyclic ene-reaction is influenced to a lesser extent. Consequently, while the pericyclic ene-reaction was by far the most favorable pathway *in vacuo*, the differences shrink for a polar environment. Again, although the computed barriers vary to some extent, all methods agree that the barrier heights of the first step of the ene- and S_EAr mechanism differ only by 3-4 kcal/mol. Additionally, all methods predict that the TS_{ene} is lower in energy than $TS1_{S_EAR}$. They also agree that the barriers of the two remaining reaction mechanisms are considerably higher in energy. Within the pericyclic ene-mechanism the final product is formed from intermediate **3** by a keto-enol tautomerization. As it will not take place *in vacuo,* but in solution, the same arguments previously discussed for the final step of the S_EAr mechanism apply. We therefore conclude that this step is not kinetically important as well. Hence, the barrier (TS_{ene}) leading to the intermediate **3** is predicted to be the rate determining step of the pericyclic ene-mechanism. This is underlined by the fact that the high barrier (> 30 kcal/mol) prevents any backwards reactions from **3** at room temperature. This may lead to an initial mixture of ketone and phenol forms in aprotic solvents if the product tautomerization is slow. The mechanistical pathway of the ene reaction is showcased in Figure 3.

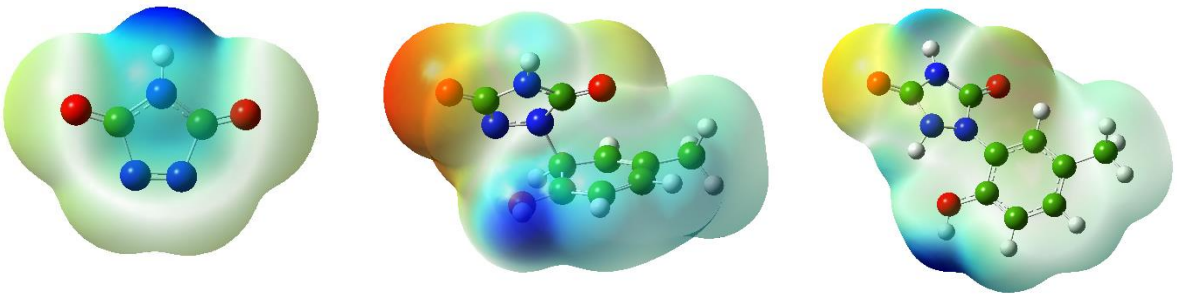

HTAD σ-complex product

Figure 2: Surface charge-densities for the three selected stationary points of the S_EAr reaction path.

We are mainly interested in the reaction of PTAD derivatives with tyrosine within aqueous solutions. Hence, it is necessary to investigate if a water molecule catalyzes the various mechanisms differently. For the S_EAr mechanism (Figure 1) a protic solvent simplifies the formation of a 6-membered transition structure for the proton transfer connecting the σ-complex with the final product due to the excess of solvent molecules. To estimate this barrier height, we computed the $TS2_{S_EAR}$ (6-mem) using a water molecule as model for the bridging molecule. In such calculations it is very important to balance the stabilization effects of the single water molecule for the different stationary points. This becomes obvious from variations in the charge distributions for selected stationary points of the S_EAr mechanism which are summarized in Figure 2. They indicate that the charges of the carbonyl moieties vary considerably along the S_EAr mechanism. Hence, if the additional water molecule forms a hydrogen bridge to the carbonyl center whose charge varies mostly along the reaction path the reactivity of the HTAD should be influenced. For the $TS2_{S_EAR}$ (6-mem) transition state, however, the water molecule has to be involved in the 6-membered transition state. Consequently, the relative energy of this transition state is overestimated if the water molecule is connected with the carbonyl group for all other stationary points. The error is reduced because we include polarization effects by the PCM continuum approach. To estimate connected error bars, we give two relative energies for the $TS2_{S_EAR}$ (6-mem) transition state. As an upper bound for the barrier height of the second step of the S_EAr mechanism we give the relative energy of the $TS2_{S_EAR}$ (6-mem) transition state with respect to the fragments HTAD + cresol in which the water molecule is placed at one carbonyl group of HTAD. This can be considered as an upper bound because due to the position of the water molecule the fragments should be more stabilized than the $TS2_{S_EAR}$ (6-mem) transition state. As a lower bound we give the relative energy of the transition state with respect to the fragment energy without the stabilization through the additional water molecule. This is a lower bound, because only the $TS2_{S_EAR}$ (6-mem) transition state undergoes some stabilization due to the water molecule. Comparable values are given for the relative energies with respect to the CT-complex. They will be discussed below. The same considerations hold for a seven-membered ring of the $TS_{Solvent}$ (see Figure 3). For all other stationary points, the additional water molecule is always positioned at the carbonyl group possessing the highest negative partial charge. The structures of the various stationary points are given in the Figure S3. The various conceivable mechanisms are visualized including the error estimates in Figures 3,4 and 5.

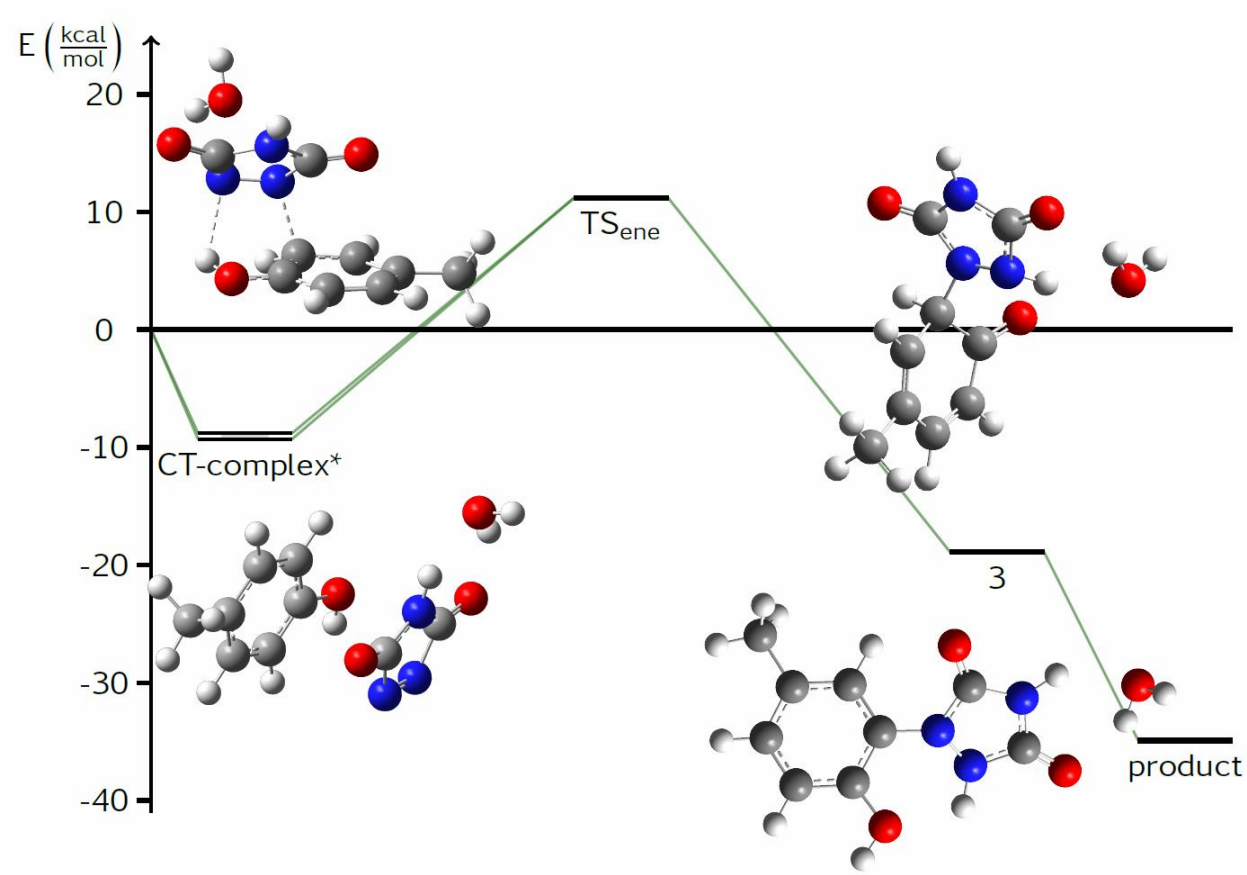

Figure 3: Intermediates and transition states present in the ene-reaction pathway of the reaction of HTAD with *p*-cresol. Energies are taken from Table 1 at the CCSD(T) + PCM + H_2O level of theory. (*): For the CT-complex two energy estimates depending on the placement of the explicit water molecule have been calculated. They serve as an upper and lower error bound. For more information, see text and Table 1.

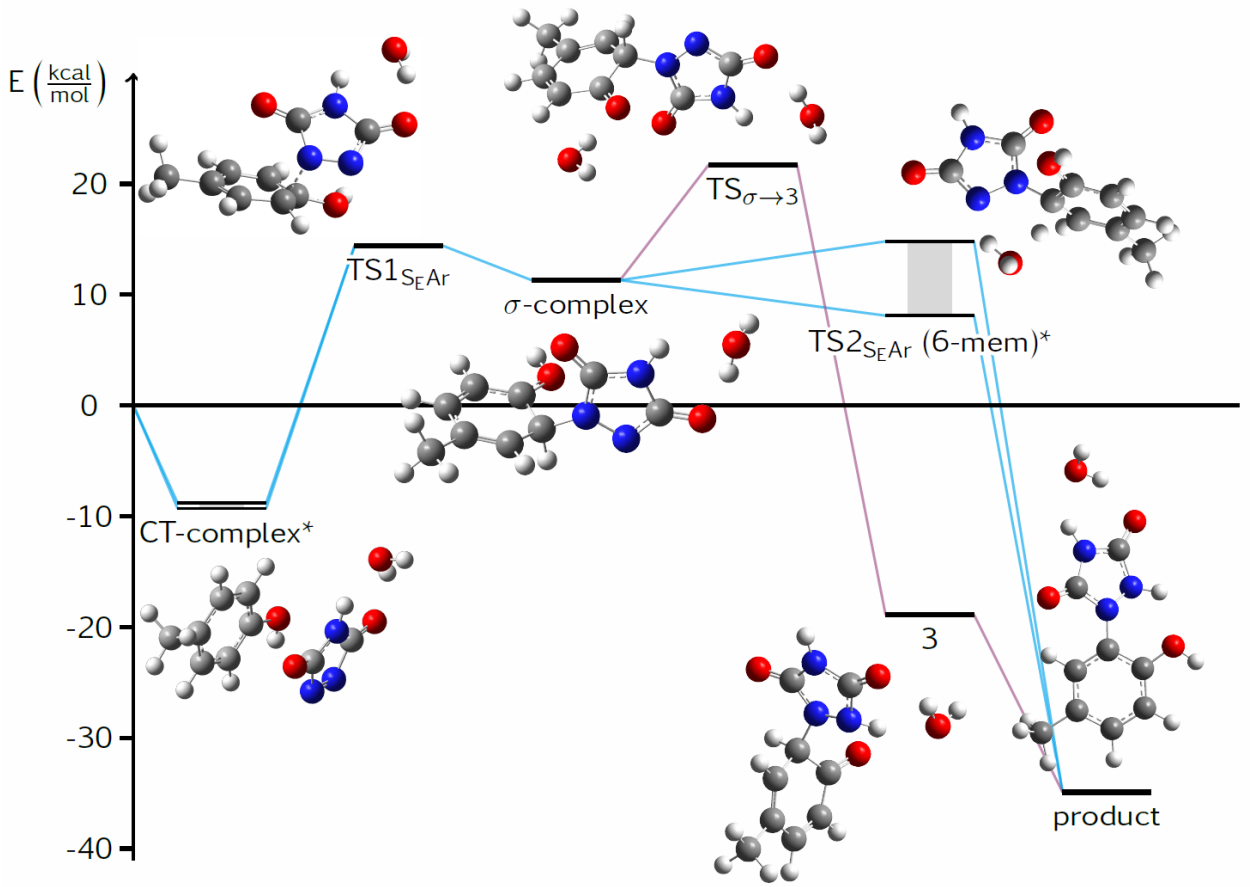

Figure 4: Intermediates and transition states occurring for the S_EAr mechanisms of the bioconjugation reaction. Energies are taken from Table 1 at the CCSD(T) + PCM + H_2O level of theory. (*): For the CT-complex and $TS2_{S_EAR}$ (6-mem) two energy estimates depending on the placement of the explicit water molecule have been calculated. They serve as an upper and lower error bound (grey bar for $TS2_{S_EAR}$ (6-mem)). For more information, see text and Table 1.

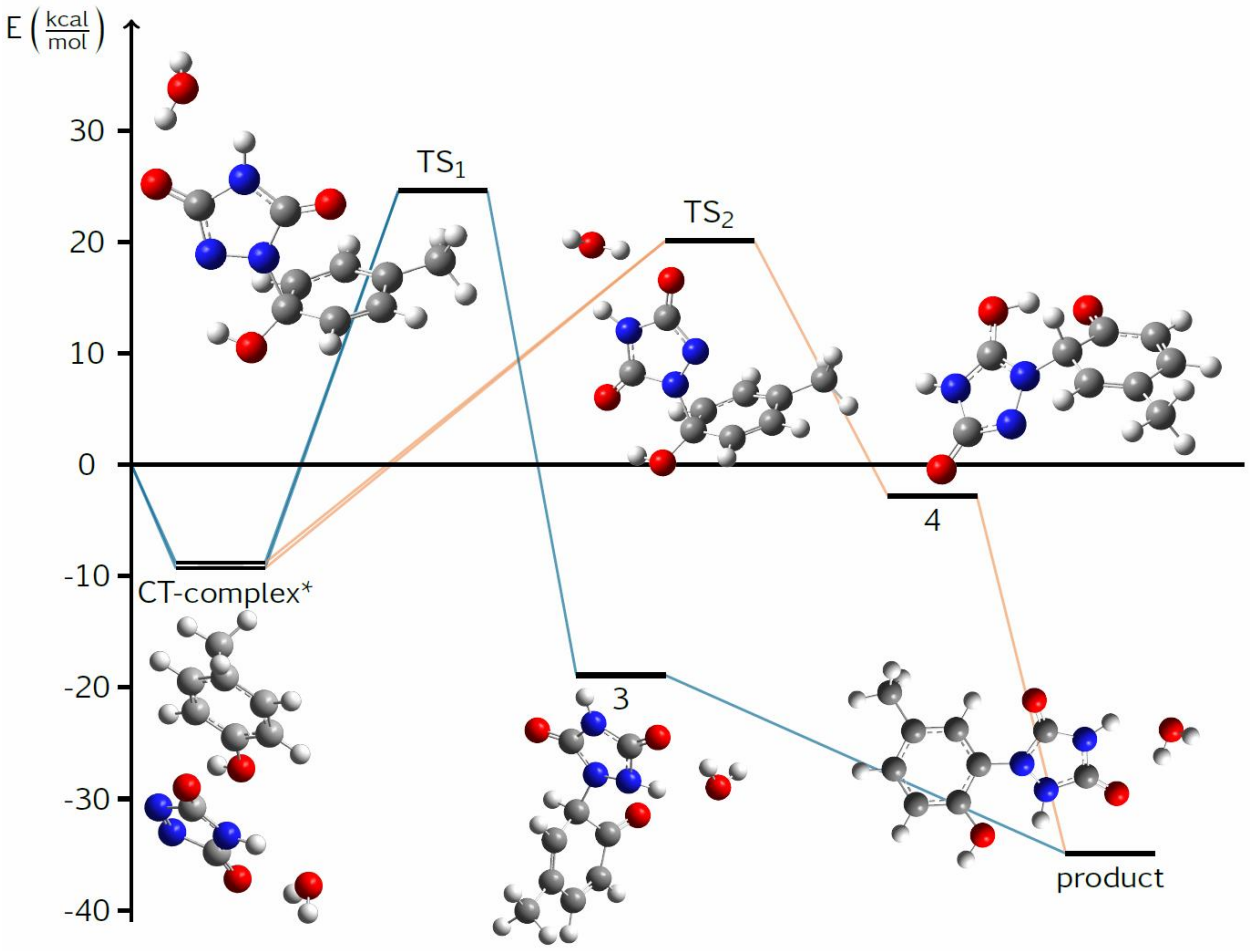

Figure 5: Intermediates and transition states present in the step-wise reaction pathways of the reaction of HTAD with *p*-cresol. Energies are taken from Table 1 at the CCSD(T) + PCM + H_2O level of theory, except for **4**, which the CCSD(T) + PCM energy difference is displayed. (*): For the CT-complex two energy estimates depending on the placement of the explicit water molecule have been calculated. For more information, see text and Table 1.

According to ωB97xD and CCSD(T) the stability of the CT-complex does not change much if a water molecule is added to the carbonyl group of HTAD. Without any water (see second column of Table 1 and Table S5) the computed values vary between -6 kcal/mol (ωB97xD) and -10 kcal/mol (CCSD(T)) while -7 and -10 kcal/mol are computed if one water molecule is added (Table 3). This is expected because the stability of the CT-complex results from dispersion effects which are not strongly influenced by the additional water molecule. One might expect that the additional water molecule stabilizes the σ-complex with respect to the CT-complex but also these effects are small. Using water as a model for the bridging molecule ωB97xD computations predict the lower and upper bounds for the height of the $TS2_{S_EAR}$ (6-mem) transition state with respect to the CT-complex to be 7 and 12 kcal/mol, respectively (see third column of Table 1 and Table S6). The CCSD(T) approach predicts a higher barrier (17.4 and 23.6 kcal/mol for lower and upper limit, respectively) while CASPT2(14,14) comes to a similar conclusion as ωB97xD (7.5 and 14.1 kcal/mol, respectively). All approaches predict that the barrier for the proton transfer connecting the σ-complex with intermediate **3** is higher than the $TS2_{S_EAR}$ (6-mem) transition state, i.e. the reaction

will proceed along the latter TS. Summarizing, all theoretical approaches agree that the formation of the σ-complex remains the rate-dependent step in protic solvents because the heights of the $TS1_{S_EAR}$ barrier with respect to the CT-complex is considerably higher (ωB97xD: 23.2 kcal/mol; CCSD(T): 23.2 kcal/mol; CASPT2 (14,14) 20.6 kcal/mol) than the subsequent barriers.

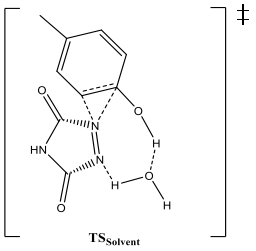

Figure 6:
Seven membered transition state of the ene-reaction involving one water molecule as bridge.

As expected, the relative transition state energies of the pericyclic ene mechanism with respect to the CT-complex are only slightly influenced by an additional water molecule. We also tested if a bridging water molecule leads to a lower barrier for the ene mechanism ($TS_{Solvent}$ Figure 6), however, the seven-membered transition state is similarly high or even higher than the six-membered concerted transition state without an additional water molecule. Consequently, also in protic solvents the barrier for the formation of the intermediate **3** remains so high, that only a slow reaction is expected. This agrees well with the available experimental data, as we will discuss below. Finally, the additional water molecule also does not change the barriers heights of the step-wise mechanisms (see Figure 5) with respect to the CT-complex so that they remain considerably less favorable than the pericyclic ene- or the S_EAr reaction (see Figures 3 and 4). Summarizing, also for protic solvents the pericyclic ene-reaction remains slightly more favorable than the S_EAr reaction, however the computed barriers (20-21 kcal/mol) are quite high so that only very slow reactions are expected.

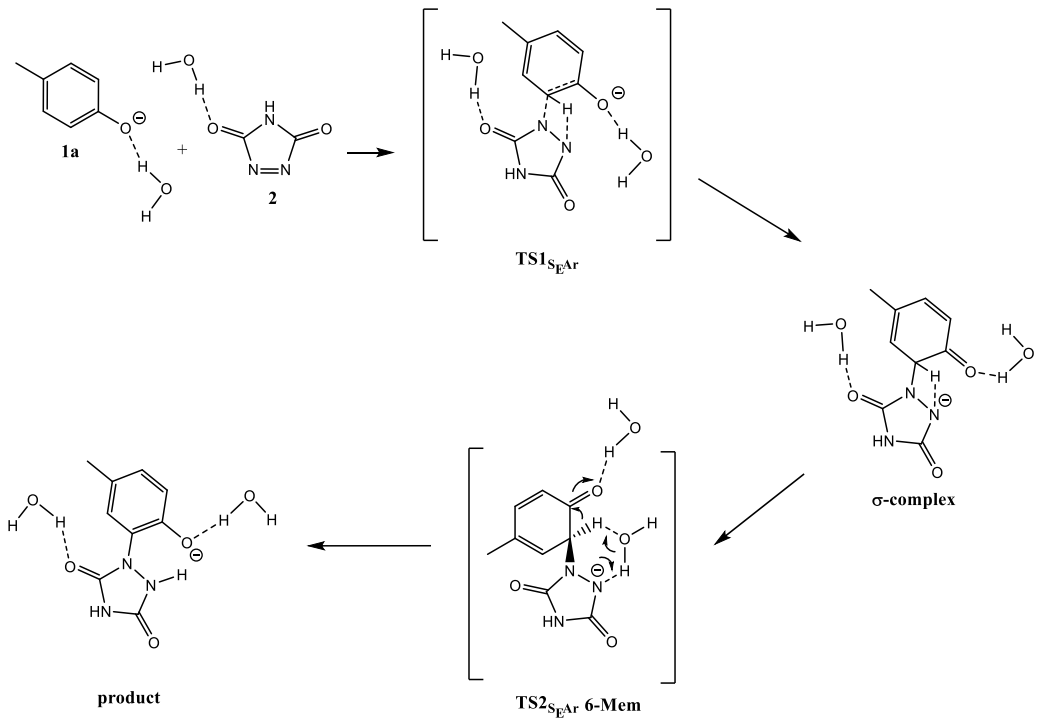

Figure 7: S_EAr reaction pathways for the reaction of *p*-cresolate (**1a**) and HTAD (**2**). The water molecules shall only indicate to which centers the hydrogen bond is formed. The computed molecular geometries can be seen in Figure 8 and Figure S4.

CT-complex	$TS1_{S_EAR}$	σ-complex	$TS2_{S_EAR}$ (6-mem)	product
[1] -14.8 [2] -13.6	-11.0 (3.8)	-33.5 (-18.7)	[1] -17.5 (-2.7) [2] -22.0 (-6.4)	-53.2 (-38.4)

[1] relative energies with respect to the fragments or CT-complex (in parenthesis) in which the water molecule is positioned at the carbonyl group

[2] relative energies with respect to fragments or CT-complex (in parenthesis) which are not stabilized by a water molecule.

Table 2: Relative energies [kcal/mol] with respect to the fragments (to the CT-complex) of the stationary points of the S_EAr mechanism of the reaction of TAD with *p*-cresolate including two explicit water molecules. Calculations were performed at the ωB97xD/aug-cc-pVDZ level of theory. Additional polarization effects of the water environment were included via the PCM approach. For more information, see Table 3 and text.

Experimental data indicates that PTAD also reacts with cresolate or phenolate,[39] for which no ene-reaction is possible. To investigate differences between cresol and cresolate we also characterize the S_EAr reactions of *p*-cresolate with HTAD (Figure 7 and Table 2). The corresponding computed structures are given in Figure S4 and the comprehensive mechanism is visualized in Figure 8. As for the previous calculations we used one water molecule which is either attached to the carbonyl group or used to form the 6-membered

transition state $\mathrm{TS2}_{\mathrm{S_EAR}}$ (6-mem). A lower and upper estimate of this barrier are given as well. Because negatively charged oxygen species are often troublesome if solvent effects are only described by a continuum approach,[63] we added another water molecule which for the whole reaction remained at the oxygen center of the cresol moiety. We only employed the ωB97xD/aug-cc-pVDZ approach because the system became too large for the computationally more expensive approaches. Furthermore, the previous computations for cresol have shown that ωB97xD/aug-cc-pVDZ gives the right trends. According to our calculations, all the barriers nearly disappear (Table 2). The barrier for the formation of the σ-complex is predicted to be only about 4 kcal/mol with respect to the CT-complex. Due to the increased reactivity of the cresolate the formation of the σ-complex is already exothermic and even the $\mathrm{TS2}_{\mathrm{S_EAR}}$ (6-mem) transition state is slightly more stable than the CT-complex (between -3 and -6 kcal/mol). Nevertheless, it is about 12-16 kcal/mol higher in energy than the σ-complex. Consequently, the second step of the S_EAr mechanism becomes the rate determining step of the overall reaction. However, this step is still considerably faster than the reaction of the cresol with HTAD because this barrier is 5-9 kcal/mol lower than the lowest barrier in the reaction of the cresol (12- 16 vs. 21 kcal/mol (ωB97xD), respectively). Furthermore, even if a large amount of the released energy is dissipated after the formation of the σ-complex, the system will still have a considerable amount of excess energy which additionally accelerates the formation of the product. Taking this into account by inserting the computed barriers into the Arrhenius equation, it can be estimated that the rate constant of the cresolate reaction is about 10^4-10^7 times larger than that of the cresol reaction. This nicely matches the available experimental results as we will discuss below.

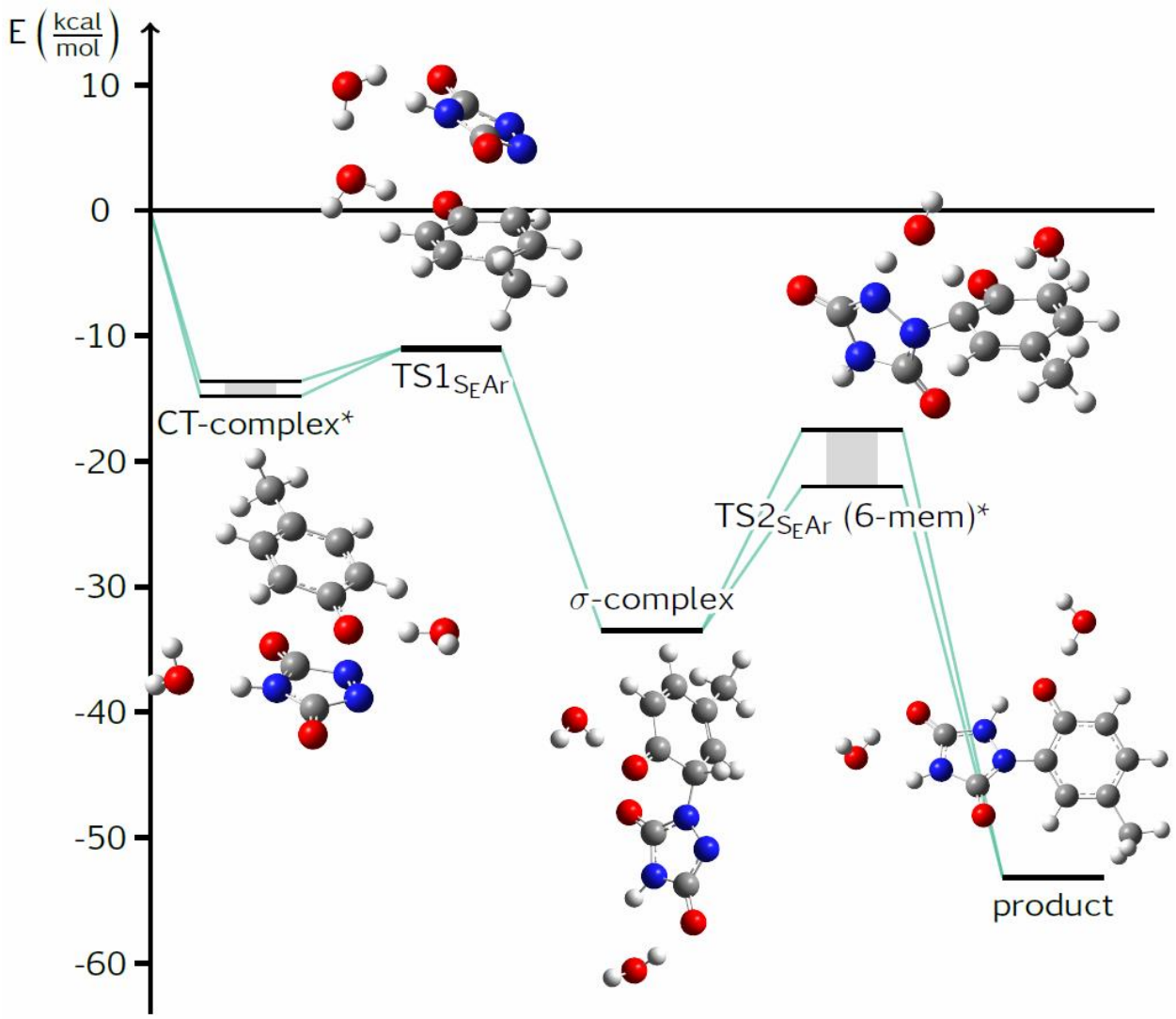

Figure 8: Intermediates and transition states present in the S_EAr reaction of HTAD with the *p*-cresolate anion. Energies are taken from Table 2 at the ωB97xD level of theory. Solvent effects are accounted for by the inclusion of two water molecules as well as by using the PCM approach. (*): For the CT-complex and $TS2_{S_EAR}$ (6-mem) two energy estimates depending on the placement of the explicit water molecule have been calculated. They serve as an upper and lower error bound (grey bar for $TS2_{S_EAR}$ (6-mem)). For more information, see text and Table 2.

The HTAD reaction with propene and vinyl-alcohol

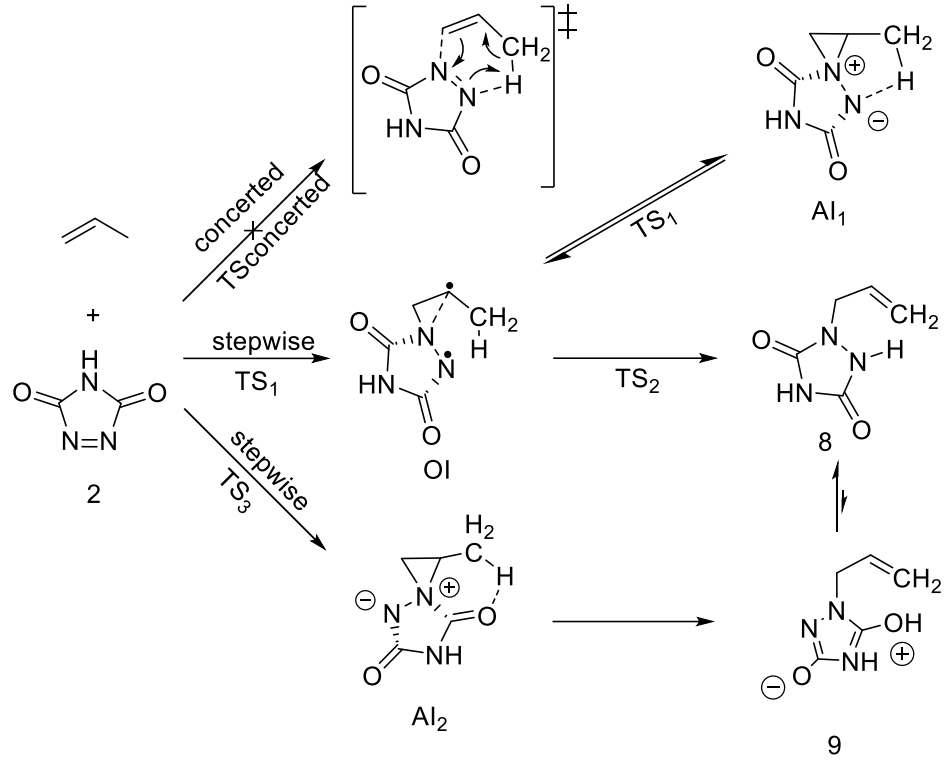

Figure 9: An overview of the possible mechanistic pathways of the ene-reaction of TAD with propene, adapted from Houk and Leach.[34]

Our computations predict that for the reaction of HTAD with cresol the ene and S_EAr mechanism possess barriers of similar heights while the barriers of the stepwise reactions are considerably higher in energy. In contrast for the reactions of PTAD with xylene, mesitylene or propene radical mechanisms were found.[19] To elucidate the underlying differences we compared the reactions of HTAD with cresol with its reaction with vinyl-alcohol or propene. For vinyl alcohol the same chemical motive as *p*-cresol is involved in the ene-reaction but the aromatic ring is lacking. For propene the aromatic ring is missing and additionally the alcohol-moiety is replaced by an alkyl group. The propene reaction was already carefully characterized by Houk and co-workers.[32, 34] We simply repeated these computations using CCSD(T), CASPT2 and ωB97xD, all in combination with the aug-cc-pVDZ basis, to have consistent data for all systems. To investigate possible solvent effects, we performed optimizations *in vacuo* and included solvent effects through the PCM continuum model for water. Solvent-dependent changes in the ene-reaction of RTAD with Alkenes were investigated by various groups.[64-67] The mechanisms computed by Houk and co-workers for the propene reaction are sketched in Figure 9. The corresponding computed structures of the stationary points are summarized in the SI (Figure S5). To name the various stationary points we adopted the labels coined by Houk and co-workers. For vinyl alcohol we investigated all similar possibilities by replacing the CH_2-moity of the methyl group by an oxygen atom. The results obtained for propene are summarized in Table 3 (in vacuum) and Table 4 (in solvent) while those computed for vinyl alcohol are collected in Table 5.

	ωB97xD	CCSD(T)	CCSD $\mathcal{T}_1$ diagnostic	CASPT2(14,14)
CT-complex	-5.3	-5.6	0.016	-6.8
TS_1	10.3	9.1	0.019	9.6
OI	5.8	2.8	0.024	6.1
TS_2	0.6	4.3	0.026	0.9
8	-43.3	-34.5	0.016	-30.5
AI_1	-13	-4.4	0.017	-5.9
TS_3	15.8	15	0.024	10.4
AI_2	-11.3	-2.8	0.016	-4.2
9	-11	-3.3	0.027	-13.5

Table 3: Results of quantum chemical calculations of the reaction of TAD with propene *in vacuo*. All geometries were optimized at the ωB97xD/aug-cc-pVDZ level of theory. For more information, see Table 1 and text. Please note, the geometry "OI" is not a minimum on the ωB97xD PES. The structure was thus obtained from an unrestricted MP2/aug-cc-pVDZ optimization.

	CCSD(T)	CASPT2(14,14)
CT-complex	-4.4	-5.9
TS_1	9.9	0.8
OI	3.9	-4.2
TS_2	4.4	-4.9
8	-34.7	-49.7
AI_1	-9.7	-9.4
TS_3	15.2	10.8
AI_2	-8.4	-12.4
9	-14.3	-32.5

Table 4: Results of quantum chemical calculations of the reaction of TAD with propene including implicit solvation at the PCM level of theory for the solvent water. Structures have been obtained at the ωB97xD/aug-cc-pVDZ level of theory in vacuum. For more information, see Table 1 and text. We note that structure OI was not a stationary point on both the ωB97xD and uMP2 PES when the PCM implicit solvation model is used.

We could not identify a transition state for the concerted pathway in the case of propene and TAD. Accordingly, we assume that the barrier of the corresponding reaction path is too high. Our computations predict two possible mechanisms. The first reaction mechanism (Figure 9) proceeds to OI via TS_1 and then to compound **8** via TS_2. Using ωB97xD or CCSD(T) TS_1 and TS_2 are higher in energy than OI so that these approaches also predict a two-step mechanism. This is in line with the MP2 computations of Houk and coworkers.[32]

However, in accordance with the Lewis structure given in Figure 9 the $\mathcal{T}_1$-diagnostics indicate some multi-reference character for various stationary points. This effect is especially pronounced for the intermediate OI and the transition state TS_2. Because this might lead to errors in the single-configuration approaches (CCSD(T) and ωB97xD) we also employed the multi-reference method CASPT2(14,14). In contrast to the

single reference approaches it predicts the OI to be higher in energy than the following transition state geometry TS_2. Hence CASPT2(14,14) predicts that after passing TS_1 the reaction proceeds to compound **8** without any further barrier, i.e. a one-step mechanism with TS_1 as barrier maximum is computed. It is important to note that the absolute differences within the predictions are too small for a definitive answer. CCSD(T) computes the TS_2 to be 1-2 kcal/mol higher than the OI intermediate while CASPT2(14,14) calculates it to be 1-2 kcal/mol lower in energy, i.e. the differences in the predictions are only about 3-4 kcal/mol.

All approaches agree that the reaction process along TS_1 becomes more complicated due to the minimum AI. Our computations predict that the path from the reactants to OI but also the path to AI_1 proceed *via* TS_1 or at least via structurally and energetically very similar transition states. This finding originates from IRC calculations performed at the B3LYP, MP2, and ωB97xD level of theory *in vacuo*. Employing MP2 or ωB97xD, IRC calculations starting from TS_1 connect the reactants with the AI_1 intermediate. Employing B3LYP a connection between the reactants and the OI intermediate is computed. Using ωB97xD or unrestricted ωB97xD, no OI minimum geometry is located at all, which would be in line with the CASPT2(14,14) computations. The unrestricted MP2 method locates the OI geometry, but only as an intermediate structure along the reaction path to AI_1. These ambiguous results indicate that the PES of the reaction is very complex and probably possesses various flat minima. This flatness also explains why the different theoretical approaches comes to different conclusions. Our computations find no direct transition state between AI_1 and **8** which supports a previously assumption that the AI_1 is an impasse in the TAD reaction.[34, 68-69]

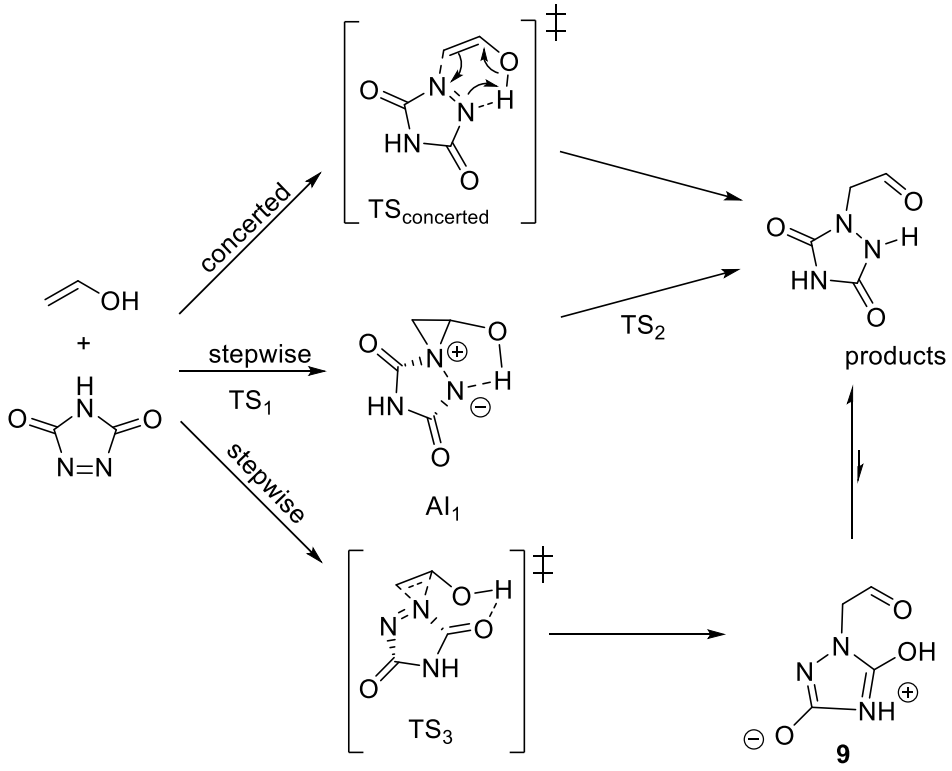

Figure 10: Overview of the possible mechanistic pathways of the ene-reaction of HTAD with vinyl-alcohol. To simplify the comparison, the stationary points are labeled according to the reaction with propene.

Finally, our computations predict that the second mechanism which proceed through TS_3 to the intermediate AI_2 and to **9** is less important. All methods agree that its barrier height is about 3-5 kcal/mol higher than the barrier height of the first mechanism running through TS_1. Please note, that the approaches predict different barrier heights for both paths but agree in the differences between both paths.

Including solvent effects, the PCM continuum approach does not change the picture. All barriers get smaller, but the relative heights remain. As for vacuum, single reference approaches predict a two-step mechanism while CASPT2(14,14) indicates a single-step mechanism. But again, the absolute differences between the various methods are too small for a definitive answer. As for vacuum also for a polar environment the ene mechanism can be ruled out because again as no transition state is found. Summarizing, our computations agree with previous experimental and theoretical findings that the ene mechanism does not take place for the reaction of HTAD and propene.

	ωB97xD	CCSD(T)	CCSD $\mathcal{T}_1$ diagnostic	CASPT2 (8,8)	ωB97xD + PCM	CCSD(T) + PCM	CASPT2(8,8) + PCM
CT-complex	-6.7	-7.3	0.017	-7.6	-5.2	-5.8	-7.1
TS_{ene}	5.7 (12.4)	5.7 (13.0)	0.021	1.9 (9.5)	5.4 (10.6)	6.0 (11.8)	0.7 (7.8)
TS_1	10.6	10.5	0.020	8.8	6.6	7.4	-1.9
AI_1	-10.4	-2.1	0.017	-2.7	-12.9	-4.3	-12.4
TS_2	-7.6	0.2	0.020	-4.4	-10.8	-1.9	-10.7
TS_3	11.7	12.3	0.023	8.0	10.7	12.3	6.6
9	-25.8	-17.4	0.019	-16.6	-34.0	-25.2	-26.5
Product	-52.4	-43.9	0.017	-43.0	-52.7	-43.6	-46.5

Table 5: Results of quantum chemical calculations of the reaction of TAD with vinyl-alcohol. The PCM implicit solvation model was used to model solvation effects in water. All geometries were optimized at the ωB97xD/aug-cc-pVDZ level of theory *in vacuo* or in PCM. Energies are given in kcal/mol relative to the separated reactants.

To investigate the question whether the aromatic ring or the OH-group leads to the strong stabilization of the ene mechanism we investigated the reaction between HTAD and vinyl alcohol. The corresponding mechanisms are indicated in Figure 10 while the relative energies of the stationary points are summarized in Table 5. It shows, that the OH-group considerably stabilizes the ene-reaction path. For vacuum this reaction path possesses a reaction barrier of about 6 kcal/mol which is about 4 kcal/mol lower in energy than the corresponding barriers of the stepwise reaction paths. If solvent effects are taken into account, however, the barriers of the ene (TS_{ene}) and the stepwise reaction (TS_1) are nearly the same, i.e. the reaction would proceed along both mechanisms. Considering, that for cresol the barrier of the ene-reaction was considerably lower (Table 1, CCSD(T) + PCM: TS_{ene} = 11 kcal/mol) than the barrier of the stepwise mechanism (Table 1, CCSD(T) + PCM: TS1 = 25 kcal/mol) it becomes obvious that the OH-group and the aromaticity contribute to the stabilization of the ene-reaction path for the reaction of cresol with HTAD. The stationary points of the stepwise reaction paths of vinyl alcohol and HTAD resemble the corresponding points of the HTAD reaction with propene.

Discussion and Conclusion

Using high-level quantum chemical approaches, we computed various possible reaction paths of the reaction of HTAD with cresol and with cresolate. Solvent effects were included to be able to interpret available experimental results which are mainly obtained in a polar protic solvent (e.g. water). Our computations come to the following conclusions: The stepwise mechanisms which take place in the reaction of PTAD and propene or aromatic hydrocarbons do not play a role of significance for the reaction of PTAD with phenol, cresol or tyrosine. For these compounds, the reaction either proceeds along the pericyclic ene- or along the S_EAr mechanism. The stabilization of the transition state of the ene-mechanism, which seems to be very high for the reaction of PTAD with propene, results due to the replacement of the CH group by the OH group but is also influenced by the aromatic ring as shown by the comparison of the reaction of vinyl alcohol with HTAD and the reaction of cresol with HTAD.

The computations of the reaction of HTAD with cresol predict that the reaction should be rather slow in aprotic as well as in protic solvents at room temperature because of the prohibitively high activation barriers of 20-21 kcal/mol for the ene-reaction. The barriers of the other possible reaction mechanisms are even higher. The barriers of the ene-reaction are slightly lower than those of the S_EAr mechanism, but the differences are too small for a definitive answer regarding which of the mechanism takes place. Central for the rationalization of the experimental results is our prediction that the barriers of the S_EAr mechanism for reaction of cresolate with HTAD are considerably lower than the corresponding barriers of the reaction with cresol. The ωB97xD/aug-cc-pVDZ approach predicts that the barrier of the rate determining step of the S_EAr-reaction ($TS1_{S_EAR}$) drops by at least about 5-9 kcal/mol (Table 3 vs. Table 4). Additionally, the intermediates have a considerable amount of excess energy because the formation of the σ-complex is already exothermic. Taking this into account the Arrhenius equation predicts that the rate constant of the cresolate reaction is about 10^5-10^7 higher than the corresponding cresol rate constant.

This strong difference nicely explains various experimental findings.[24-25, 39] The fact that no conversion is found for the reaction in pure MeCN or in a MeCN-H_2O (1:1) mixture can be explained by the high barriers in aprotic as well as protic solvents. For protic solvents, one has to take into account that PTAD rapidly decomposes in aqueous solution,[15-16] explaining the non-formation of product in water or simple aqueous media (CH_3CN:H_2O mixtures). Barbas III and co-workers could show that efficient conversion and rapid product formation is only found within different phosphate buffers around pH 7. According to our computational results, this remarkable difference can be traced back to the relative amount of phenolate in these solutions whose reaction rate constant is considerably higher. Assuming a pK_a value of about 10 for cresol and ignoring possible increased acidity by the formation of CT complex, the ratio of cresolate to cresol is concentration dependent, and will approach $\sqrt{10^{-pK_a}}$ (=10^{-5}) for concentrated solutions, although a higher degree of protolysis is possible upon dilution. Combining this lower limit for the relative concentration of cresolate anions with the above-mentioned acceleration factor for the reaction constant (10^4-10^7), the overall rate of the cresolate reaction is expected to be 0.1 - 100 times that for its non-deprotonated cresol counterpart. Hence, the measured conversion rates are expected to primarily result from the reaction of cresolate. This also explains the experimental finding that the reaction of PTAD with phenols can be accelerated if a base is added and that the conversion rates at pH 2 are considerably lower than those at pH 8-10.[24-25] It also explains the absence of product formation in neutral water. The reaction product (urazole) is itself also a weak acid (pK_a ~5), which will further raise the concentration of hydroxonium upon reaction (drop in pH), pushing the protolysis equilibrium of cresol even more to the protonated form, and significantly slowing down the TAD-click reaction, favoring the background hydrolysis reaction of TAD. In a buffered solution, however, the relative concentration of cresolate is kept at a constant, concentration-independent level, as given by the buffer formula, thus fixing the ratio of

cresolate to cresol at 10^{pH-pK_a} (i.e. approx. 1/1000 at pH 7) throughout the course of the reaction. Combining this value with the calculated acceleration factor of 10^4-10^7, the reaction of cresolate is predicted to be 10 - 10,000 times faster than the reaction of cresol. These considerations together with our calculated barriers readily explain all experimental observations for tyrosine click reactions with TADs. Our computations can also be used to explain the experimental findings that phenol compounds with unblocked para-positions also gives the para-substituted PTAD-adduct.[39] With respect to the importance of the various mechanisms our computations predict that for the reaction of cresol with HTAD the pericyclic ene-mechanism is within the energy range of the S_EAr mechanism but that the experimentally observed adduct formations ultimately result from reactions of cresolate proceeding only along the S_EAr mechanism. From our theoretical rationalization, the prediction can be made that the selectivity of the bioconjugation of different solvent-exposed tyrosine residues of a protein will not only depend on the steric hindrance, but also on the corresponding pK_a values of the tyrosines within their ordered micro-environment. pK_a values can easily shift over multiple units, giving rise to orders of magnitude difference in reactivity. The presented findings may rationalize yet unexplained selectivities satisfactorily.[30, 70-71] Experimental investigations to further substantiate these intriguing predictions are currently under way.

Supporting Information

All three-dimensional structures are collected in the Supporting Information to this report along with comprehensive information on the CASPT2, CCSD(T) and ωB97xD calculations. Detailed accounts of our investigation of the CT-complex and open-shell intermediates can be found as well.

Literature

1. Cookson, R. C.; Gilani, S. S. H.; Stevens, I. D. R., Diels-Alder Reactions of 4-Phenyl-182,4-triazoline-3,5-dione. *Journal of the Chemical Society C: Organic* 1967, (19), 1905-1909.
2. Jensen, F.; Foote, C. S., Reaction of 4-Phenyl-1,2,4-triazoline-3,5-dione with Substituted Butadienes. A Nonconcerted Diels-Alder Reaction. *Journal of the American Chemical Society* 1987, *109* (21), 6376-6385.
3. Orfanopoulos, M.; Smonou, I.; Foote, C. S., Intermediates in the Ene Reactions of Singlet Oxygen and N-Phenyl-1,2,4-triazoline-3,5-dione with Olefins. *Journal of the American Chemical Society* 1990, *112* (9), 3607-3614.
4. Gillis, B. T.; Hagarty, J. D., The Reaction of 4-Phenyl-l,2,4-triazoline-3,5-dione with Conjugated Dienes. *Journal of Organic Chemistry* 1967, *32* (2), 330-330.
5. Hall, J. H.; Jones, M. L., Reactions of azodiones with electron-rich alkenes. 1, 2, 4-Triazoline-3, 5-diones and vinyl ethers. *The Journal of Organic Chemistry* 1983, *48* (6), 822-826.
6. Hall, J. H., Interaction of electron-deficient 1,2,4-triazoline-3,5-diones with electron-rich polyalkoxybenzenes. *The Journal of Organic Chemistry* 1983, *48* (10), 1708-1712.

7. Kinart, W. J.; Kinart, C. M.; Oszczeda, R.; Tran, Q. T., Studies on the Catalysis by Lithium Perchlorate of Reactions of Aromatic Amines with Diethyl Azodicarboxylate and Naphtalen-2-ol with 4-phenyl-1,2,4-triazoline-3,5-dione. *Catalysis Letters* 2005, *103* (3), 185-189.
8. Zhang, J. W.; Xu, J. H.; Cheng, D. J.; Shi, C.; Liu, X. Y.; Tan, B., Discovery and enantiocontrol of axially chiral urazoles via organocatalytic tyrosine click reaction. *Nature Communications* 2016, *7*.
9. Changotra, A.; Das, S.; Sunoj, R. B., Reversing Enantioselectivity Using Noncovalent Interactions in Asymmetric Dearomatization of beta-Naphthols: The Power of 3,3 ' Substituents in Chiral Phosphoric Acid Catalysts. *Organic Letters* 2017, *19* (9), 2354-2357.
10. Algar, W. R.; Prasuhn, D. E.; Stewart, M. H.; Jennings, T. L.; Blanco-Canosa, J. B.; Dawson, P. E.; Medintz, I. L., The Controlled Display of Biomolecules on Nanoparticles: A Challenge Suited to Bioorthogonal Chemistry. *Bioconjugate Chemistry* 2011, *22* (5), 825-858.
11. Boutureira, O.; Bernardes, G. J. L., Advances in Chemical Protein Modification. *Chemical Reviews* 2015, *115* (5), 2174-2195.
12. Fujita, M.; Matsushima, H.; Sugimura, T.; Tai, A.; Okuyama, T., Asymmetric addition of an electrophile to naphthalenes promoted and stereodirected by alcohol. *Journal of the American Chemical Society* 2001, *123* (13), 2946-2957.
13. Reaney, M. J. T.; Liu, Y. D.; Taylor, W. G., Gas chromatographic analysis of Diels-Alder adducts of geometrical and positional isomers of conjugated linoleic acid. *Journal of the American Oil Chemists Society* 2001, *78* (11), 1083-1086.
14. Naik, A.; Alzeer, J.; Triemer, T.; Bujalska, A.; Luedtke, N. W., Chemoselective Modification of Vinyl DNA by Triazolinediones. *Angewandte Chemie-International Edition* 2017, *56* (36), 10850-10853.
15. Roy, N.; Lehn, J. M., Dynamic Covalent Chemistry: A Facile Room-Temperature, Reversible, Diels-Alder Reaction between Anthracene Derivatives and N-Phenyltriazolinedione. *Chemistry - An Asian Journal* 2011, *6* (9), 2419-2425.
16. Sato, S.; Nakamura, K.; Nakamura, H., Tyrosine-Specific Chemical Modification with in Situ Hemin-Activated Luminol Derivatives. *Acs Chemical Biology* 2015, *10* (11), 2633-2640.
17. Sasaki, T.; Kanemats.K; Hayakawa, K., Studies on Heteroaromaticity. Part XLVIII. Cycloaddition Reactions of 4-Phenyl-l,2,4-triazoline-3,5-dione with Seven-membered Ring Unsaturated Compounds and Photochemical Behaviour of the Adducts. *Journal of the Chemical Society C: Organic* 1971, (11), 2142-2147.
18. Breton, G. W.; Newton, K. A., Further studies of the thermal and photochemical Diels-Alder reactions of N-methyl-1,2,4-triazoline-3,5-dione (MeTAD) with naphthalene and some substituted naphthalenes. *Journal of Organic Chemistry* 2000, *65* (10), 2863-2869.

19. Breton, G. W.; Hoke, K. R., Application of Radical Cation Spin Density Maps toward the Prediction of Photochemical Reactivity between N-Methyl-1,2,4-triazoline-3,5-dione and Substituted Benzenes. *The Journal of Organic Chemistry* 2013, *78* (10), 4697-4707.
20. Ulmer, L.; Siedschlag, C.; Mattay, J., Functionalization of 60 fullerene and of 60 fullerene monoadducts by photochemical cycloaddition of 4-methyl-1,2,4-triazoline-3,5-dione. *European Journal of Organic Chemistry* 2003, (19), 3811-3817.
21. Risi, F.; Alstanei, A. M.; Volanschi, E.; Carles, M.; Pizzala, L.; Aycard, J. P., Photo addition of aliphatic ethers to 4-methyl-1,2,3-triazoline-3,5-dione: Application to the synthesis of functionalized crown ethers and mechanism. *European Journal of Organic Chemistry* 2000, (4), 617-626.
22. Eyles, D.; Anderson, C.; Ko, P.; Jones, A.; Thomas, A.; Burne, T.; Mortensen, P. B.; Norgaard-Pedersen, B.; Hougaard, D. M.; McGrath, J., A sensitive LC/MS/MS assay of 250H vitamin D-3 and 250H vitamin D-2 in dried blood spots. *Clinica Chimica Acta* 2009, *403* (1-2), 145-151.
23. Christie, W. W., Gas chromatography mass spectrometry methods for structural analysis of fatty acids. *Lipids* 1998, *33* (4), 343-353.
24. Ban, H.; Gavrilyuk, J.; Barbas, C. F., Tyrosine Bioconjugation through Aqueous Ene-Type Reactions: A Click-Like Reaction for Tyrosine. *Journal of the American Chemical Society* 2010, *132* (5), 1523-1525.
25. Ban, H.; Nagano, M.; Gavrilyuk, J.; Hakamata, W.; Inokuma, T.; Barbas, C. F., Facile and Stabile Linkages through Tyrosine: Bioconjugation Strategies with the Tyrosine-Click Reaction. *Bioconjugate Chemistry* 2013, *24* (4), 520-532.
26. Bauer, D. M.; Ahmed, I.; Vigovskaya, A.; Fruk, L., Clickable Tyrosine Binding Bifunctional Linkers for Preparation of DNA–Protein Conjugates. *Bioconjugate Chemistry* 2013, *24* (6), 1094-1101.
27. McKay, Craig S.; Finn, M. G., Click Chemistry in Complex Mixtures: Bioorthogonal Bioconjugation. *Chemistry & Biology* 2014, *21* (9), 1075-1101.
28. Billiet, S.; De Bruycker, K.; Driessen, F.; Goossens, H.; Van Speybroeck, V.; Winne, J. M.; Du Prez, F. E., Triazolinediones enable ultrafast and reversible click chemistry for the design of dynamic polymer systems. *Nat Chem* 2014, *6* (9), 815-821.
29. De Bruycker, K.; Billiet, S.; Houck, H. A.; Chattopadhyay, S.; Winne, J. M.; Du Prez, F. E., Triazolinediones as Highly Enabling Synthetic Tools. *Chemical Reviews* 2016, *116* (6), 3919-3974.
30. Ortiz-Soto, M. E.; Ertl, J.; Mut, J.; Adelmann, J.; Le, T. A.; Shan, J.; Te; Schlosser, A.; Engels, B.; Seibel, J., Product-oriented chemical surface modification of a levansucrase (SacB) via an ene-type reaction. *Chemical Science* 2018, *9* (24), 5312-5321.
31. Nabarun, R.; Jean-Marie, L., Dynamic Covalent Chemistry: A Facile Room-Temperature, Reversible, Diels–Alder Reaction between Anthracene Derivatives and N-Phenyltriazolinedione. *Chemistry – An Asian Journal* 2011, *6* (9), 2419-2425.

32. Chen, J. S.; Houk, K. N.; Foote, C. S., The nature of the transition structures of triazolinedione ene reactions. *Journal of the American Chemical Society* 1997, *119* (41), 9852-9855.
33. Lu, X., Can the nitroso Ene reaction proceed concertedly? *Organic Letters* 2004, *6* (16), 2813-2815.
34. Leach, A. G.; Houk, K. N., Diels-Alder and ene reactions of singlet oxygen, nitroso compounds and triazolinediones: transition states and mechanisms from contemporary theory. *Chemical Communications* 2002, (12), 1243-1255.
35. Rigby, J. H., [6+4] Cycloaddition Reactions. *Organic Reactions* 1996, *49*, 331.
36. Rigby, J. H.; Chouraqui, G., First intramolecular 6+4 cycloaddition of tropone and a furan moiety: Rapid entry into a highly functionalized ingenane skeleton. *Synlett* 2005, (16), 2501-2503.
37. Kim, D. K.; O'Shea, K. E., The reaction of N-methyl-1,2,4-triazoline-3,5-dione with tetracyclopropylethylene. Formation of an unusual meso-ionic product and its rearrangement to the diazetidine. *Journal of the American Chemical Society* 2004, *126* (3), 700-701.
38. Barbas, C. F. I. Tyrosine bioconjugation through aqueous ene-like reactions. 2011.
39. Barbas, C. F. I.; Ban, H.; Gavrilyuk, J. Tyrosin Bioconjugation through aqueous ene-like reactions. 30.06.2011, 2011.
40. Peric, M.; Engels, B.; Peyerimhoff, S. D., Ab initio investigation of the vibronic structure of the C2H spectrum: Computation of the vibronically averaged values for the hyperfine coupling constants. *Journal of Molecular Spectroscopy* 1991, *150* (1), 70-85.
41. Breton, G. W.; Suroviec, A. H., Intermediacy of a Persistent Urazole Radical and an Electrophilic Diazenium Species in the Acid-Catalyzed Reaction of MeTAD with Anisole. *Journal of Organic Chemistry* 2016, *81* (1), 206-214.
42. Lee, C.; Yang, W.; Parr, R. G., Development of the Colle-Salvetti correlation-energy formula into a functional of the electron density. *Physical Review B* 1988, *37* (2), 785-789.
43. Becke, A. D., Density-functional exchange-energy approximation with correct asymptotic behavior. *Physical Review A* 1988, *38* (6), 3098-3100.
44. Becke, A. D., Density-functional thermochemistry. III. The role of exact exchange. *The Journal of Chemical Physics* 1993, *98* (7), 5648-5652.
45. Kendall, R. A.; Jr., T. H. D.; Harrison, R. J., Electron affinities of the first-row atoms revisited. Systematic basis sets and wave functions. *The Journal of Chemical Physics* 1992, *96* (9), 6796-6806.
46. Chai, J. D.; Head-Gordon, M., Long-range corrected hybrid density functionals with damped atom-atom dispersion corrections. *Physical Chemistry Chemical Physics* 2008, *10* (44), 6615-6620.
47. Frisch, M. J.; Trucks, G. W.; Schlegel, H. B.; Scuseria, G. E.; Robb, M. A.; Cheeseman, J. R.; Scalmani, G.; Barone, V.; Mennucci, B.; Petersson, G. A.; Nakatsuji, H.; Caricato, M.; Li, X.; Hratchian, H. P.; Izmaylov, A. F.; Bloino, J.; Zheng, G.; Sonnenberg, J.

L.; Hada, M.; Ehara, M.; Toyota, K.; Fukuda, R.; Hasegawa, J.; Ishida, M.; Nakajima, T.; Honda, Y.; Kitao, O.; Nakai, H.; Vreven, T.; Montgomery, J. A.; Peralta, J. E.; Ogliaro, F.; Bearpark, M.; Heyd, J. J.; Brothers, E.; Kudin, K. N.; Staroverov, V. N.; Kobayashi, R.; Normand, J.; Raghavachari, K.; Rendell, A.; Burant, J. C.; Iyengar, S. S.; Tomasi, J.; Cossi, M.; Rega, N.; Millam, J. M.; Klene, M.; Knox, J. E.; Cross, J. B.; Bakken, V.; Adamo, C.; Jaramillo, J.; Gomperts, R.; Stratmann, R. E.; Yazyev, O.; Austin, A. J.; Cammi, R.; Pomelli, C.; Ochterski, J. W.; Martin, R. L.; Morokuma, K.; Zakrzewski, V. G.; Voth, G. A.; Salvador, P.; Dannenberg, J. J.; Dapprich, S.; Daniels, A. D.; Farkas, Ö.; Foresman, J. B.; Ortiz, J. V.; Cioslowski, J.; Fox, D. J., Gaussian09 Revision E.01.

48. Cheron, N.; Jacquemin, D.; Fleurat-Lessard, P., A qualitative failure of B3LYP for textbook organic reactions. *Physical Chemistry Chemical Physics* 2012, *14* (19), 7170-7175.

49. Lindh, R.; Malmqvist, P. Å.; Veryazov, V.; Widmark, P.-O.; others, *Multiconfigurational Quantum Chemistry*. John Wiley & Sons: 2016.

50. Lee, T. J.; Taylor, P. R., A diagnostic for determining the quality of single-reference electron correlation methods. *International Journal of Quantum Chemistry* 1989, *36* (S23), 199-207.

51. Pless, V.; Suter, H. U.; Engels, B., Ab initio study of the energy difference between the cyclic and linear forms of the C6 molecule. *Journal of Chemical Physics* 1994, *101* (5), 4042-4048.

52. Engels, B.; Peyerimhoff, S. D., The hyperfine coupling constants of the X 3-sigma-states of NH Influence of polarization functions and configuration space on the description of spin polarization. *Molecular Physics* 1989, *67* (3), 583-600.

53. Andersson, K.; Malmqvist, P. A.; Roos, B. O.; Sadlej, A. J.; Wolinski, K., Second-order perturbation theory with a CASSCF reference function. *Journal of Physical Chemistry* 1990, *94* (14), 5483-5488.

54. Andersson, K.; Malmqvist, P. Å.; Roos, B. O., Second-order perturbation theory with a complete active space self-consistent field reference function. *The Journal of Chemical Physics* 1992, *96* (2), 1218-1226.

55. Aquilante, F.; De Vico, L.; Ferré, N.; Ghigo, G.; Malmqvist, P.-A.; Neogrády, P.; Pedersen, T. B.; Pitoňák, M.; Reiher, M.; Roos, B. O.; Serrano-Andrés, L.; Urban, M.; Veryazov, V.; Lindh, R., MOLCAS 7: The Next Generation. *Journal of Computational Chemistry* 2010, *31* (1), 224-247.

56. Rintelman, J. M.; Adamovic, I.; Varganov, S.; Gordon, M. S., Multireference second-order perturbation theory: How size consistent is "almost size consistent". *Journal of Chemical Physics* 2005, *122* (4).

57. Kuhrau, M.; Stadler, R., Low temperature modification of polymers by triazolinediones, 2: On the mechanism of the electrophilic aromatic substitution with 4-substituted 1,2,4-triazoline-3,5-dion. *Makromolekulare Chemie - Macromolecular Chemistry and Physics* 1990, *191* (8), 1787-1798.

58. Settels, V.; Schubert, A.; Tafipolsky, M.; Liu, W.; Stehr, V.; Topczak, A. K.; Pflaum, J.; Deibel, C.; Engel, V.; Fink, R. F.; Engels, B., Identification of Ultrafast Relaxation Processes As a Major Reason for Inefficient Exciton Diffusion in Perylene-Based Organic Semiconductors. *Journal of the American Chemical Society* 2014, *136*, 9327-9337.
59. Walter, C.; Kramer, V.; Engels, B., On the applicability of time-dependent density functional theory (TDDFT) and semiempirical methods to the computation of excited-state potential energy surfaces of perylene-based dye-aggregates. *International Journal of Quantum Chemistry* 2017, *117* (6).
60. Brückner, C.; Engels, B., A Theoretical Description of Charge Reorganization Energies in Molecular Organic P-Type Semiconductors. *Journal of Computational Chemistry* 2016, *37* (15), 1335-1344.
61. Liao, M. S.; Lu, Y.; Parker, V. D.; Scheiner, S., DFT calculations and spectral measurements of charge-transfer complexes formed by aromatic amines and nitrogen heterocycles with tetracyanoethylene and chloranil. *Journal of Physical Chemistry A* 2003, *107* (42), 8939-8948.
62. Brückner, R., *Reaktionsmechanismen: Organische Reaktionen, Stereochemie, Moderne Synthesemethoden*. Spektrum Akademischer Verlag: 2009.
63. Helten, H.; Schirmeister, T.; Engels, B., Model calculations about the influence of protic environments on the alkylation step of epoxide, aziridine, and thiirane based cysteine protease inhibitors. *Journal of Physical Chemistry A* 2004, *108* (38), 7691-7701.
64. Roubelakis, M. M.; Vougioukalakis, G. C.; Angelis, Y. S.; Orfanopoulos, M., Solvent-Dependent Changes in the Ene Reaction of RTAD with Alkenes: The Cyclopropyl Group as a Mechanistic Probe. *Organic Letters* 2006, *8* (1), 39-42.
65. Vougioukalakis, G. C.; Roubelakis, M. M.; Alberti, M. N.; Orfanopoulos, M., Solvent-Dependent Changes in the Triazolinedione–Alkene Ene Reaction Mechanism. *Chemistry – A European Journal* 2008, *14* (31), 9697-9705.
66. Acevedo, O.; Jorgensen, W. L., Advances in quantum and molecular mechanical (QM/MM) simulations for organic and enzymatic reactions. *Accounts of chemical research* 2009, *43* (1), 142-151.
67. Acevedo, O.; Squillacote, M. E., A New Solvent-Dependent Mechanism for a Triazolinedione Ene Reaction. *The Journal of Organic Chemistry* 2008, *73* (3), 912-922.
68. Squillacote, M. E.; Garner, C.; Oliver, L.; Mooney, M.; Lai, Y.-L., Photochemical Generation of Aziridinium Imides: Are AIs Bystanders or Perpetrators in the Ene Reaction? *Organic Letters* 2007, *9* (26), 5405-5408.
69. Vougioukalakis, G. C.; Orfanopoulos, M., Mechanistic Studies in Triazolinedione Ene Reactions. *Synlett* 2005, *2005* (05), 0713-0731.
70. Hu, Q. Y.; Allan, M.; Adamo, R.; Quinn, D.; Zhai, H. L.; Wu, G. X.; Clark, K.; Zhou, J.; Ortiz, S.; Wang, B.; Danieli, E.; Crotti, S.; Tontini, M.; Brogioni, G.; Berti, F., Synthesis of a well-defined glycoconjugate vaccine by a tyrosine-selective conjugation strategy. *Chemical Science* 2013, *4* (10), 3827-3832.

71. Hu, Q. Y.; Berti, F.; Adamo, R., Towards the next generation of biomedicines by site-selective conjugation. *Chemical Society Reviews* 2016, *45* (6), 1691-1719.